Journal of Membrane Science 563 (2018) 31–42

Contents lists available at ScienceDirect

Journal of Membrane Science

journal homepage: www.elsevier.com/locate/memsci

Polyvinylidene fluoride membrane modification via oxidant-induced dopamine polymerization for sustainable direct-contact membrane distillation

Nick Guan Pin Chew[a,b], Shanshan Zhao[b], Chandresh Malde[c], Rong Wang[b,d,*]

[a] Interdisciplinary Graduate School, Nanyang Technological University, Singapore 639798, Singapore
[b] Singapore Membrane Technology Centre, Nanyang Environment and Water Research Institute, Nanyang Technological University, Singapore 637141, Singapore
[c] Johnson Matthey Technology Centre, Reading RG4 9NH, United Kingdom
[d] School of Civil and Environmental Engineering, Nanyang Technological University, Singapore 639798, Singapore

ARTICLE INFO

Keywords:
Membrane distillation
Surfactant
Oxidant-induced
Polydopamine
Superoleophobic

ABSTRACT

Porous hydrophobic polyvinylidene fluoride (PVDF) membranes have been extensively used in direct-contact membrane distillation (DCMD) processes. However, these PVDF membranes are vulnerable to membrane fouling and pore wetting in low surface tension feeds, restricting its application for water recovery from challenging industrial wastewaters. Therefore, it is of paramount importance to engineer fouling- and wetting-resistant MD membranes for robust long-term applications. In this study, a superoleophobic composite hollow fiber membrane with sandwich structure has been developed via accelerated oxidant-induced polydopamine (PDA) deposition on both the outer and inner surfaces of a commercial hydrophobic PVDF membrane under slightly acidic conditions (pH = 5). The modified surface prevents organics adhesion ascribing to its underwater superoleophobicity while the unmodified pores remain hydrophobic for vapor transport. The long-term robustness of the PDA-decorated membrane in highly saline feeds containing low surface tension contaminants has been evaluated via bench-scale DCMD experiments. In contrast to the pristine PVDF membrane, the PDA-decorated membrane exhibits excellent fouling- and wetting-resistant properties in different surfactant solutions as well as oil-in-water emulsion. The PDA-decorated membrane has also been used for seawater desalination, during which it maintains a stable flux and high salt rejection rate. Furthermore, the PDA-decorated membrane presents a flux enhancement of up to 70% over the pristine PVDF membrane in 3.5 wt% NaCl solution at 333 K. This study demonstrates the potential of the PDA-decorated membrane for extended DCMD applications such as water recovery from industrial wastewater containing low surface tension substances.

1. Introduction

Membrane distillation (MD) is a continuous thermal-driven desalination process based on the vapor-liquid equilibrium [1–3]. In this process, water vapor molecules from the warm saline feed transport through a porous hydrophobic membrane and condense into highly purified distillate on the cold permeate side, driven by the water vapor pressure difference associated with the temperature gradient across the membrane. MD has been proposed as a promising candidate for water recovery from highly saline feeds over conventional pressure-driven membrane processes due to its merits of low sensitivity to feed salinity, moderate operating conditions, and ability to utilize low-grade thermal energy that is abundantly available within many industries [4–6].

In the MD process, the porous hydrophobic membrane is a crucial element for efficient vapor transport and preventing liquid permeation from the saline feed to the distillate. Hence, conventional MD membranes are typically fabricated from hydrophobic polymeric materials that include polypropylene, polyvinylidene fluoride (PVDF), and polytetrafluoroethylene. These membranes have shown stable performances for treating relatively clean feeds that contain mostly salt. However, they are vulnerable to membrane fouling and pore wetting when used to treat challenging feeds that contain hydrophobic (e.g. oil) and/or amphiphilic (e.g. surfactants) pollutants. Adsorption of these substances on the membrane surface can lower the pore liquid entry pressure or cause pore blockage, which compromises on the recovery rate and distillate quality [7]. Hence, it is paramount to develop robust MD membranes with fouling- and wetting-resistant properties. This could potentially extend the applications of the MD process to treating

* Corresponding author at: Singapore Membrane Technology Centre, Nanyang Environment and Water Research Institute, Nanyang Technological University, Singapore 637141, Singapore.
E-mail address: rwang@ntu.edu.sg (R. Wang).

https://doi.org/10.1016/j.memsci.2018.05.035
Received 11 March 2018; Received in revised form 13 May 2018; Accepted 19 May 2018
Available online 26 May 2018
0376-7388/

oil-in-water (O/W) emulsions such as produced water as well as surfactant-containing wastewaters from the textile, food, paint, polymer, cosmetic, and pharmaceutical industries, to name a few. Recent studies have provided an insight on that [7,8]. It has been suggested that omniphobic and composite membranes can provide a solution to membrane fouling and pore wetting faced in low surface tension feeds via MD [6,9–11].

Hierarchical re-entrant structures, coupled with low surface energy, can improve the anti-wetting properties of omniphobic membranes as they represent a significant energetic barrier that has to be overcome in order to transit from the metastable Cassie-Baxter state to the fully wetted Wenzel state [6,12–15]. The other approach to mitigate fouling and wetting involves creating a superhydrophilic skin layer on the top of a hydrophobic or omniphobic substrate [11,16,17]. This forms a hydration layer surrounding the superhydrophilic skin and renders the membrane surface superoleophobic under water. Besides that, incorporation of low surface energy functional groups into the hydrophilic matrix can further facilitate the detachment of hydrophobic foulants such as oil [18]. It is evident from these studies that strides have been made in improving the anti-fouling and anti-wetting properties of MD membranes. Yet, most of these surface modification techniques are often too complex for practical applications. Therefore, developing a facile technique to engineer robust MD membranes that can handle wastewaters containing low surface tension pollutants is of high priority.

Moreover, to make MD membranes commercially viable, membranes with high vapor permeability have to be developed [19]. This can be achieved through altering vapor-membrane interaction, which is one of the major physicochemical factors determining permeability [20]. Apart from that, striking a balance between high mass transfer and low heat loss is also vital in enhancing vapor permeation flux in MD operations [21]. In line with this, much effort has been focused on performing surface modification on commercially available polymeric substrates to attempt to enhance flux, which includes the immobilization of carbon nanotubes (CNT) in membrane pores [19]. CNT's excellent thermal conductivity reduces the effect of temperature polarization, which in turn brings about an increase in vapor driving force across the membrane. In addition, CNT's remarkable sorption and desorption capacity contribute favorably to water-membrane interactions. Faster removal of water vapor from the membrane pores is also possible via CNT's atomic-scale smooth surface. Similar concepts have been proposed through incorporating nanodiamond and graphene oxide within the membrane matrix [22,23]. Besides that, reducing vapor transport distance while maintaining the membrane thickness can facilitate mass transport across the membrane [21]. These works have contributed tremendously to developing MD membranes with enhanced flux, but the performances of these membranes in saline feeds containing low surface tension pollutants are found to be undesirable.

Since 2007, the mussel-inspired chemistry of dopamine has opened up avenues for numerous applications due to its unique advantages of material-independent attachment and surface post-functionalization under relatively mild conditions [24]. However, most of the surface modification techniques involving dopamine investigated thus far have proven to be laborious and time-consuming. These techniques involve numerous preparation steps, and require long hours of coating [25]. Often, the deposition of polydopamine (PDA) through these conventional techniques is non-homogenous, of low thickness, and of limited hydrophilicity. In our previous study, the coating process took more than a day to achieve the desired thickness [11]. Even so, the deposited layer presented limited hydrophilicity. Furthermore, the modified membrane was especially vulnerable to wetting in some non-ionic surfactant solutions and fouling in anionic surfactant solutions. It has been suggested that the use of oxidants, in replacement of dissolved oxygen, can overcome these limitations [26,27].

This study focuses on developing a robust MD membrane with enhanced flux for water recovery from wastewaters containing low surface tension solutes via direct-contact membrane distillation (DCMD). Specifically, a superoleophobic composite membrane with sandwich structure was fabricated through facile single-step deposition of hydrophilic PDA layer in the presence of an oxidant, namely sodium periodate (SP), on both the outer and inner surfaces of a commercial hydrophobic PVDF hollow fiber substrate. The surface chemistry and hierarchical structure of the modified PVDF membrane were studied comprehensively through a range of characterization techniques. The fouling and wetting propensities of the modified PVDF membrane were investigated via a bench-scale DCMD experimental rig by feeding a series of low surface tension saline wastewater. Its performances were analyzed and then compared against those of the pristine PVDF and

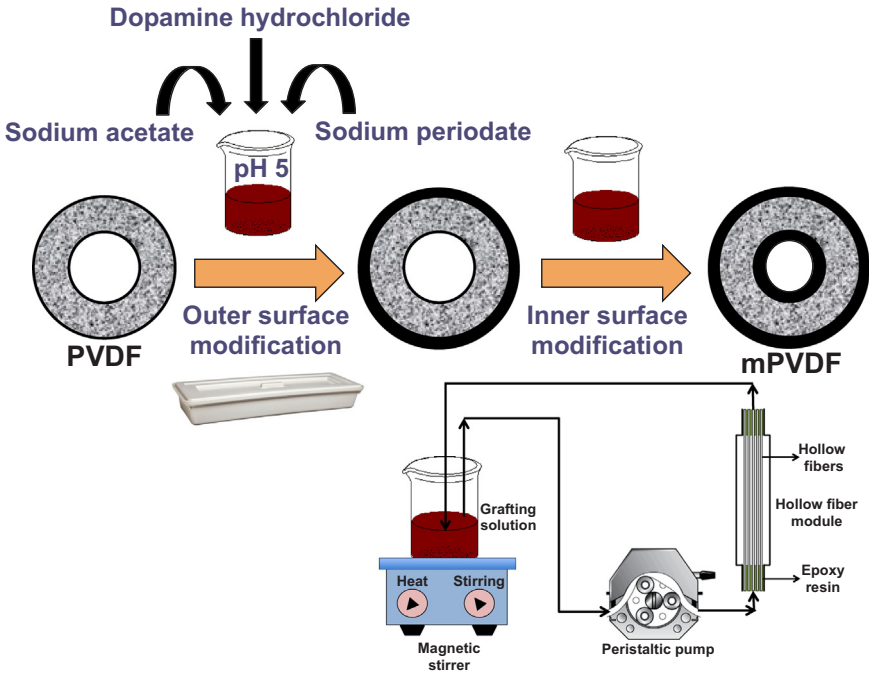

Fig. 1. Schematic of oxidant-induced deposition of PDA on the outer and inner surfaces of a PVDF hollow fiber membrane.

previously reported composite membranes to ascertain its applicability and robustness for long-term treatment of low surface tension feeds. To the best of our knowledge, this is the first report on oxidant-induced dopamine modification on a hydrophobic PVDF hollow fiber substrate for extended applications of DCMD.

2. Experimental

2.1. Materials and chemicals

Dopamine hydrochloride (DA), SP, sodium dodecyl sulfate (SDS), dodecyltrimethylammonium bromide (DTAB), petroleum, sodium hydroxide (NaOH), and hydrochloric acid (HCl) were purchased from Sigma-Aldrich (Singapore). Sodium chloride (NaCl, 99.5%), anhydrous sodium acetate, 2-propanol (IPA), and polyoxyethylenesorbitan monolaurate (Tween® 20) were purchased from Merck Millipore (Singapore). All purchased chemicals were used as received. Hydrophobic PVDF hollow fiber membranes with a nominal pore size of 27 nm were supplied by a commercial manufacturer and its properties had been reported in our previous study [7]. The received hollow fiber membranes were immersed in Milli-Q® water at 313 K for at least 3 h to get rid of chemical residues from the fabrication process. Subsequently, the membranes were dried overnight in a vacuum oven at 323 K (Heraeus Vacutherm® Oven, Thermo Fisher Scientific, Singapore). The dried membranes were then used as substrates for surface modification and as references for the DCMD performance tests. The Milli-Q® water produced by the Milli-Q® integral water purification system (Merck Millipore) had a resistivity value of 18.2 MΩ cm and was used in preparing all aqueous feed solutions.

2.2. Fabrication of composite PVDF membrane

The composite membrane was fabricated by facile deposition of PDA on both the outer and inner surfaces of a hydrophobic PVDF substrate to create a sandwich structure as illustrated in Fig. 1. The coating solution was first prepared by dissolving 2 g L^{-1} DA into 50 mM sodium acetate buffer with 20 mM SP as the oxidant [27]. The solution was adjusted with 2 M HCl to pH 5. Hereon, the coating solution will be referred to as the PDASP solution. For outer surface modification, both ends of each hollow fiber membrane were sealed to ensure that only its outer surface was modified while the membrane pores beneath the surface remained hydrophobic for vapor transport. The pristine PVDF hollow fiber membranes were partially pre-wetted with predetermined concentrations of IPA for a designated time prior to being immersed in the PDASP solution with shaking at 30 rpm (Orbital Maxi MD Humidity, OVAN, Spain) for designated times (2 h or 6 h) under ambient conditions. Hereon, the modified membranes with different deposition times will be referred to as the 2 h-mPVDF and 6 h-mPVDF membranes, respectively. Finally, the modified membranes were washed thoroughly with Milli-Q® water and dried overnight in the vacuum oven at 323 K. Lab-scale modules were prepared by sealing the dried hollow fibers in Teflon tubing with epoxy resin. A new membrane module was prepared for each experiment. The effective membrane area for each module was 35 cm^2.

To perform inner surface modification on the 2 h-mPVDF and 6 h-mPVDF membranes, freshly prepared PDASP solution was circulated in the membrane lumen by a peristaltic pump at 0.01 L min^{-1} for 1 h on a bench-scale cross-flow setup as illustrated in Fig. 1. Throughout the reaction, the PDASP solution was covered with aluminum foil and stirred at 300 rpm under ambient conditions. The membrane lumen was washed thoroughly with Milli-Q® water after modification.

2.3. Membrane characterizations

The detailed characterization procedures had been described in our previous studies [7,11]. Typically, the outer surface and cross-section morphologies of the pristine PVDF, 2 h-mPVDF, and 6 h-mPVDF membranes were characterized via a field emission scanning electron microscope (FESEM) (JSM-7200F, JEOL, Japan). The respective hollow fiber samples were freeze-fractured in liquid nitrogen and then sputter-coated with a layer of platinum by a sputter coater (JEC-3000FC, JEOL, Japan) prior to FESEM imaging. Changes in the topography and roughness of the membrane outer surface after PDA deposition were observed through an atomic force microscope (AFM) (XE-100, Park Systems, Korea) with a scan area of 5 μm by 5 μm via the non-contact mode under ambient conditions.

A Fourier transform infrared spectroscope with attenuated total reflectance mode (ATR-FTIR) (IR-Prestige-21, Shimadzu, Japan) was used to qualitatively analyze the changes in surface functional groups on the membrane after modification. 45 scans were conducted under ambient conditions in the range of 400–4000 cm^{-1} at a resolution of 4 cm^{-1}. The elemental compositions of the outer and inner surfaces of the pristine PVDF and 6 h-mPVDF membranes were examined using an X-ray photoelectron spectroscope (XPS) (Quantera II, Physical Electronics, Inc., USA) with a monochromatic Al Kα excitation source at 1486.6 eV. High-resolution spectra were collected with the X-ray source operating at 15 kV and 40 W, using pass energies of 55 eV and 224 eV for narrow and wide scans, respectively. Sampling was carried out at a takeoff angle of 45° with a spot size of 200 μm. All binding energies (BE) for the elements of interest were referenced to the adventitious C 1s core level at 284.8 eV.

An electrokinetic analyzer (SurPASS™ 3, Anton Paar, Austria) and an adjustable gap cell (20 mm × 10 mm) were employed for streaming potential measurements to investigate the surface zeta potential of the pristine PVDF and 6 h-mPVDF membranes. The pH of the electrolyte solution (1 mM NaCl) was first adjusted to pH 10 by dosing it with NaOH. Each measurement was recorded at ambient conditions and a maximum pressure difference of 600 mbar. Subsequently, the electrolyte solution was dosed with HCl in a stepwise fashion to pH 3.

The dynamic water contact angles of the outer surfaces of the pristine PVDF and 6 h-mPVDF membranes were measured by a tensiometer (DCAT11, DataPhysics, Germany) using the Wilhelmy method. To obtain accurate measurements, the lumens of the pristine PVDF and 6 h-mPVDF membranes were filled with epoxy resin and allowed to dry overnight. This was to ensure that only the outer surfaces of both membranes were in contact with the Milli-Q® water during the test procedure. Each membrane sample was measured ten times and an average value was calculated. The captive bubble method via a goniometer (Contact Angle System OCA 15EC, DataPhysics, Germany) was utilized to observe underwater oil-membrane interactions on the pristine PVDF and 6 h-mPVDF membranes.

The structural stability of the 6 h-mPVDF membrane was evaluated according to the degree of surface deterioration via ultrasonic treatment for at least 10 min in an ultrasonic bath with a frequency of 37 kHz (FB 15068, Fisher Scientific, USA).

2.4. Preparation and characterization of surfactant solutions and surfactant-stabilized petroleum-in-water emulsion

To understand the fouling and wetting propensities of the pristine and modified PVDF membranes, high salinity feeds containing low surface tension contaminants were used, which include three types of surfactant solutions and one O/W emulsion. The surfactant solutions were prepared by mixing 50 mg L^{-1} of non-ionic surfactant Tween® 20, anionic surfactant SDS, or cationic surfactant DTAB in 3.5 wt% NaCl solution, respectively. 50 mg L^{-1} is above the critical micelle concentration (CMC) for Tween® 20 and below the CMC for SDS and DTAB. The properties of these surfactant solutions can be found in our previous studies [7,11]. The 500 mg L^{-1} O/W emulsion was prepared by mixing petroleum and Tween® 20 in 3.5 wt% NaCl solution at a concentration ratio of 9:1 using a high-speed heavy-duty blender (CB15, Waring® Commercial, USA) for 3 min to obtain the desirable oil droplet

Table 1
Main compositions of the seawater used in this study.

Parameter	Value
pH	7.8 ± 0.2
Conductivity (mS cm^{-1})	48.4 ± 1.1
Dissolved oxygen (mg L^{-1})	5.5 ± 1.2
Ca (mg L^{-1})	362
Mg (mg L^{-1})	1252
Na (mg L^{-1})	10600
Cl (mg L^{-1})	18890

size. The mean oil droplet size was around 2.16 μm. Petroleum, Tween® 20, and NaCl represented the oil, surfactant, and total dissolved solids present in produced water, respectively. Fresh emulsion was prepared daily to maintain the kinetic stability of the feed for accurately demonstrating the robustness of each membrane.

2.5. Raw seawater

In order to compare the DCMD performances of the pristine and modified PVDF (2 h-mPVDF and 6 h-mPVDF) membranes in real applications, a systematic study was carried out against seawater samples collected from a local desalination plant. The seawater samples were

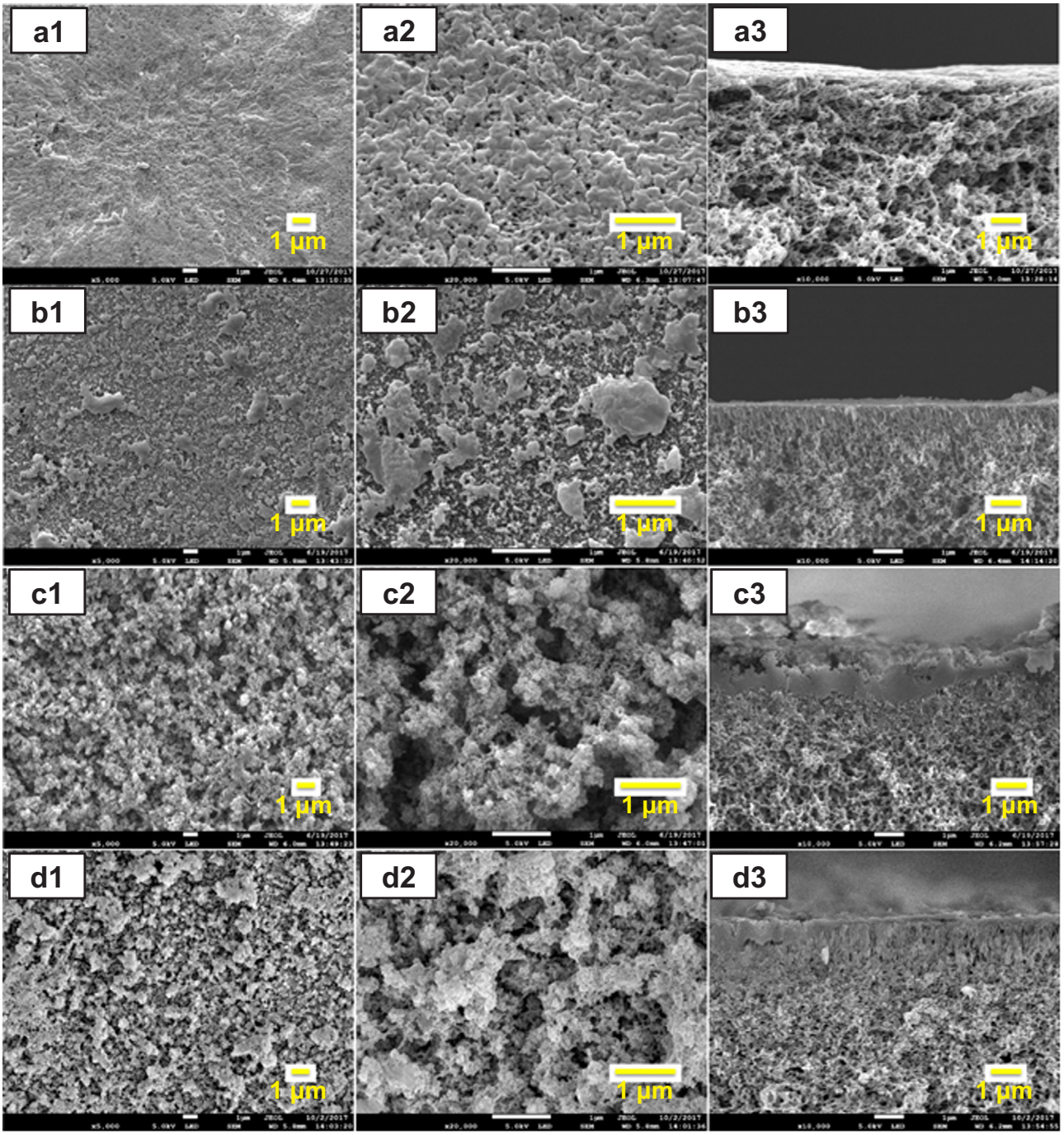

Fig. 2. FESEM images of the outer surface morphologies of the pristine PVDF (a1 and a2), 2 h-mPVDF (b1 and b2), 6 h-mPVDF (c1 and c2), and ultrasonicated 6 h-mPVDF (d1 and d2) membranes. FESEM images of the cross-section morphologies of the pristine PVDF (a3), 2 h-mPVDF (b3), 6 h-mPVDF (c3), and ultrasonicated 6 h-mPVDF (d3) membranes.

stored at ambient conditions and used as received. No pre-treatment was carried out prior to the respective experiments. The water quality of the seawater is listed in Table 1. The detailed analytical measurement methods were described in our previous study [28].

2.6. DCMD performance tests

The fouling and wetting behaviors of the mPVDF membranes were systematically studied and compared with the pristine PVDF and previously reported PDA/PEI modified membranes [11]. The experiments were carried out on a bench-scale DCMD setup as illustrated in our previous study [9]. The saline feed solution was controlled at 333 K by a heater and circulated on the shell side of the hollow fibers at a flow rate of 0.7 L min^{-1}, while Milli-Q® water was cooled down to 293 K and circulated on the lumen side in a countercurrent flow configuration at a flow rate of 0.25 L min^{-1}. The permeate was collected into an overflow tank placed on a digital balance connected to a computerized data logging system. The permeate flux was recorded 1 h after the start of the experiment, when the system had stabilized. Minimal pressure was applied to the feed side to facilitate observation of NaCl permeation, if any. The temporal changes in permeate conductivity were monitored by a conductivity probe to an accuracy of ± 0.1 μS cm^{-1}. During the experiments, all of the tubes and membrane modules were insulated with insulation foam to prevent heat loss.

3. Results and discussion

3.1. Observations of membrane surface morphology

The outer surface and cross-section morphologies of the pristine PVDF, 2 h-mPVDF, and 6 h-mPVDF membranes were observed using FESEM and the images are shown in Fig. 2. The changes in surface morphology were apparent after PDA deposition. As shown in Fig. 2(a1) and (a2), the pristine PVDF membrane surface was smooth with abundant pores. The oxidant-induced polymerization of dopamine deposited a thin layer of agglomerates, as large as 1 μm, on the pristine PVDF membrane surface after 2 h (as observed in Fig. 2(b1)–(b3)), which thoroughly covered the highly porous surface. When the coating duration was extended to six hours, minute PDA particles were deposited on the PVDF membrane surface to create a hierarchical structure with high surface roughness as corroborated by the roughness parameters listed in Table 2. High surface roughness contributes greatly to membrane superhydrophilicity as evidenced by the low water contact angle, 13.2 ± 2.4°, of the 6 h-mPVDF membrane [29–31]. The surface hierarchical structure, coupled with superhydrophilicity, can potentially impart underwater superoleophobic properties to the modified membrane, which will be discussed in Section 3.3. Fig. 2(b3) and (c3) reveal that the deposited layer did not permeate into the bulk of the PVDF substrate, hence ensuring that the membrane pores beneath the surface remained hydrophobic for vapor transport. Moreover, the deposited layer was structurally stable. It remained intact and minimal changes to its surface morphology were observed even after ultrasonication as evidenced by Fig. 2(d1)-(d3).

Table 2
Surface roughness parameters and water contact angles of the pristine PVDF and 6 h-mPVDF membranes.

Membranes	Roughness			Water contact angle (deg.)
	R_a[a] (nm)	R_q[b] (nm)	R_z[c] (nm)	
PVDF	25.6	31.9	258.3	109.5 ± 1.2
6 h-mPVDF	113.0	145.0	895.9	13.2 ± 2.4

[a] Average roughness.
[b] Root-mean-squared roughness.
[c] Ten point average roughness.

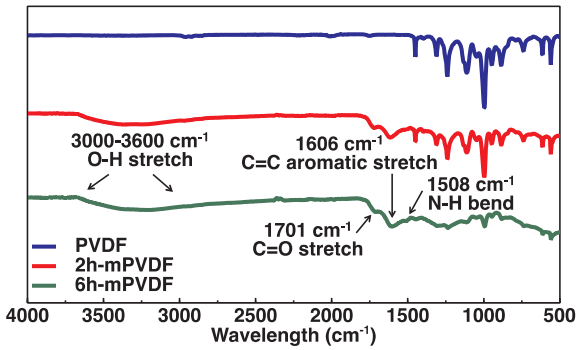

Fig. 3. ATR-FTIR spectra of the outer surfaces of the pristine PVDF, 2 h-mPVDF, and 6 h-mPVDF membranes. Transmittance was normalized against the CF peak.

The pore size distributions of the pristine PVDF and 6 h-mPVDF membranes are illustrated in Fig. A1. While both membranes have distinct bimodal distributions, they have contrasting mean pore sizes. The pristine PVDF membrane has a larger mean pore size (0.027 μm) as compared to the 6 h-mPVDF membrane (0.018 μm), which is consistent with the FESEM images. This is indicative of the alteration in intrinsic pore structure of the pristine PVDF membrane after oxidation-induced polymerization of dopamine on its surface. Introduction of PDA onto the membrane surface would have restricted some of the bigger pores and covered the smaller pores found in the pristine PVDF membrane. Consequently, the 6 h-mPVDF membrane is expected to be less susceptible to fouling and pore wetting owing to the additional protection offered by the deposited layer.

3.2. Characterizations of membrane surface chemistry

The changes in surface functional groups of the membrane after PDA deposition was characterized by ATR-FTIR and the spectra are presented in Fig. 3. Two distinct absorption peaks at 1508 cm^{-1} and 1606 cm^{-1} were detected on the mPVDF membranes, which are assigned to the primary amine N-H bending and C=C aromatic stretch within the PDA structure, respectively [32]. The absorption peak observed at 1701 cm^{-1} on the mPVDF membranes is indicative of carbonyl/carboxyl groups, suggesting the successful deposition of carboxyl-functional groups during the accelerated oxidative process induced by SP under slightly acidic conditions [27,32]. This in turn rendered the mPVDF membrane surface more hydrophilic than the previously reported PDA/PEI coated membrane [11].

The surface chemical compositions of the pristine PVDF and oxidant-induced PDA coated membranes were compared via XPS analysis as shown in Table 3 and Fig. 4. It can be seen that the outer and inner surface elemental compositions of both membranes were dissimilar. The F 1s and Cl 2p peaks that were initially present on both the outer and inner surfaces of the pristine PVDF membrane could not be observed on either surface of the 6 h-mPVDF membrane after modification. The synchronous appearance of the O 1s, N 1s, and I 3d peaks on both the outer and inner surfaces of the 6 h-mPVDF membrane mirrored the successful deposition of PDA. The significant increase in atomic

Table 3
Elemental compositions (in atomic percentage) of the outer (OS) and inner (IS) surfaces of the pristine PVDF and 6 h-mPVDF membranes.

Membrane	C 1s	F 1s	O 1s	Cl 2p	N 1s	I 3d	N/C	O/C
PVDF-OS	54.9	37.2	1.9	6.0	–	–	–	0.03
6 h-mPVDF-OS	65.5	–	25.5	–	7.8	1.2	0.12	0.39
PVDF-IS	49.1	42.5	0.4	8.0	–	–	–	0.01
6 h-mPVDF-IS	68.6	–	23.9	–	7.2	0.4	0.10	0.35

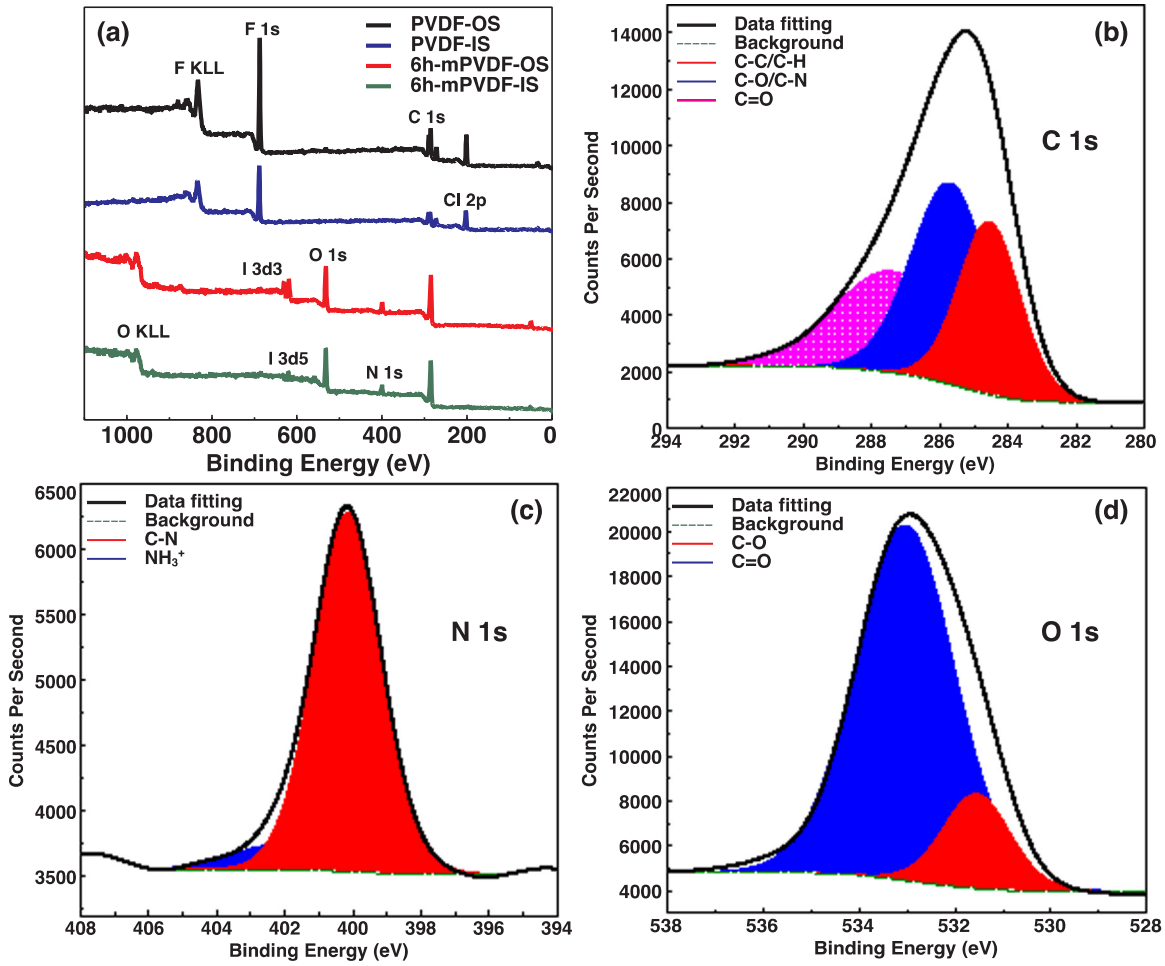

Fig. 4. (a) XPS survey scan spectra of the outer (OS) and inner (IS) surfaces of the pristine PVDF and 6 h-mPVDF membranes. Deconvolution spectra of (b) C 1s, (c) N 1s, and (d) O 1s on the outer surface of the 6 h-mPVDF membrane (the inner surface coating time is 1 h).

concentration of O 1s after surface modification was consistent with the ATR-FTIR results, suggesting the formation of carboxyl-functional groups and oxidative o-quinone cleavage during oxidant-induced polymerization of dopamine [27,32,33]. The O/C ratios of the outer and inner surfaces of the 6 h-mPVDF membrane were 0.39 and 0.35, respectively. These ratios were noticeably higher than dopamine's stoichiometric ratio of 0.25 as reported by Lee et al. [34], which was a further proof of the oxidative effect initiated through the addition of SP. Previous studies reported that prolonged oxidation time could lead to the loss of amine groups and decarboxylation of pyrrole moieties, resulting in a smaller N/C ratio [27,32]. However, the N/C ratios of both the outer and inner surfaces of the 6 h-mPVDF membrane were similar despite their contrasting deposition times. This was possible through the suppression of the oxidative breakdown process by preparing fresh coating solution every 2 h for outer surface modification. As shown in the deconvolution spectra of the 6 h-mPVDF membrane in Fig. 4(b)-(d), the C 1s core-level spectrum revealed three peak components at BE of 284.8 eV, 285.8 eV, and 288.5 eV, which were assigned to the chemical states of C-C/C-H, C-O/C-N, and C = O, respectively. The N 1s core-level spectrum was curve-fitted with two components, one at a BE of 400.1 eV for the chemical state of C-N and the other at a BE of 402.3 eV for the chemical state of protonated amine-functional group. The O 1s spectrum presented two peak components at BE of 531.6 eV and 533.9 eV, which were assigned to the C-O and C = O of the carboxylic acid moieties, respectively. The XPS analysis results were consistent with the structural components of the SP-oxidized PDA as proposed by previous studies [27,32].

The surface charge property of a membrane is very important for MD applications because the electrostatic interaction between foulants and the membrane surface influences membrane fouling and wetting behaviors [35]. Therefore, the pH dependence of surface zeta potential of the 6 h-mPVDF membrane was studied and compared with the pristine PVDF membrane via streaming potential measurements. As shown in Fig. 5, the pristine PVDF was mostly negatively charged throughout the tested pH range, which was consistent with data found in literature [36]. In comparison with the pristine PDVF membrane, the 6 h-mPVDF membrane was less negatively charged. Amine- and phenolic hydroxyl-functional groups endowed PDA with amphoteric properties. The former protonated from –NH to $–NH_2^+$ at low pH while the latter dissociated from –OH to $–O^-$ at high pH [37,38]. Apart from that, its negative charge at high pH could also be ascribed to dissociation of the carboxyl-functional groups.

3.3. Underwater oil-membrane interactions

With reference to Table 2, the pristine PVDF membrane was in-air hydrophobic and the 6 h-mPVDF membrane was in-air superhydrophilic with water contact angle values of 109.5 ± 1.2° and 13.2 ± 2.4°, respectively. The 6 h-mPVDF membrane's superhydrophilicity could be attributed to the deposition of polar amine-, hydroxyl-, and carboxyl-functional groups during surface modification. In addition, the hierarchical structures with high surface roughness of the 6 h-mPVDF membrane were instrumental in augmenting its intrinsic wetting properties [12]. The addition of a liquid droplet (i.e.

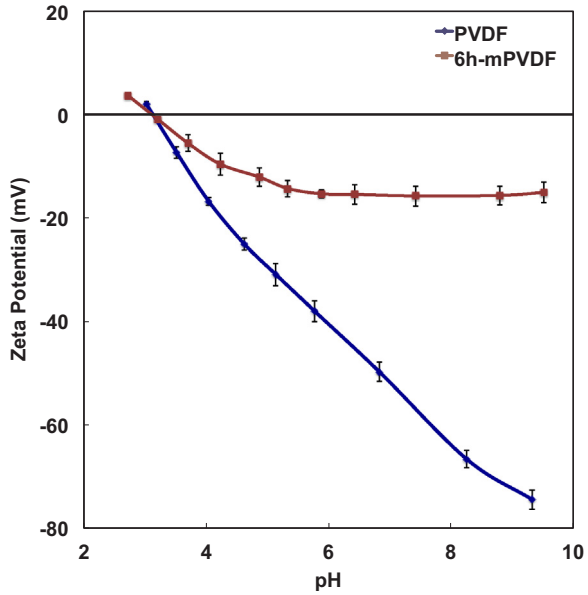

Fig. 5. Surface zeta potentials of the pristine PVDF and 6 h-mPVDF membranes as a function of pH. 1 mM NaCl was used as the background electrolyte solution.

petroleum droplet) to textured surfaces can lead to a Cassie-Baxter state that supports a composite interface, which facilitates non-wetting and easy droplet roll-off [12]. The underwater captive bubble method was applied to probe further into the mechanics of the Cassie-Baxter state at the oil-water-solid interface in the hierarchical structure on the 6 h-mPVDF membrane surface. A petroleum droplet, Milli-Q® water, and a piece of 6 h-mPVDF membrane represented the oil, water, and solid phase, respectively. Video clips (Video S1 and S2) showing the underwater interactions between the petroleum droplet and different membrane surfaces are provided as supplementary material. The relevant captured images of the underwater interactions are illustrated in Fig. 6. Upon contact, the petroleum droplet immediately adhered onto the pristine PVDF membrane surface and spread across the entire surface within 15 s. In contrast, there was neither deformation of the petroleum droplet nor petroleum residue on the 6 h-mPVDF membrane surface upon contact. Similar observations were recorded even when there was forced contact between the petroleum droplet and the 6 h-mPVDF membrane surface, attesting its underwater superoleophobic property. The hierarchical structure, coupled with surface superhydrophilicity, imparted the underwater superoleophobic property of the modified membrane. In such a scenario, an interfacial hydration layer was formed on the membrane surface and trapped water within the hierarchical structure, prohibiting oil attachment on the surface. The oil adhesion-resistant property of the 6 h-mPVDF membrane renders it a suitable candidate for effective oil-water separation via DCMD.

Supplementary material related to this article can be found online at http://dx.doi.org/10.1016/j.memsci.2018.05.035.

3.4. Membrane performance in DCMD tests

3.4.1. Saline feeds with anionic, cationic, and non-ionic surfactants

To investigate the intrinsic MD performances of the modified PVDF membranes, baseline tests were first conducted using 3.5 wt% NaCl solution as feed. The permeate flux and conductivity over a period of 24 h of the 2 h-mPVDF-O (only outer surface modification was performed) and 2 h-mPVDF (outer and inner surface modifications were performed) membranes were recorded and compared with the pristine PVDF and previously reported PDA/PEI coated membranes, which are presented in Fig. 7. It was evident that all of the four membranes exhibited stable fluxes and conductivities throughout the operation. The deposited PDA layer did not provide additional mass transfer resistance to vapor transport across the membrane pores and there was no salt breakthrough. The permeate flux of the 2 h-mPVDF membrane was the highest, presenting approximately 70% flux enhancement over the pristine PVDF membrane. The average permeate fluxes of the pristine PVDF, PDA/PEI, 2 h-mPVDF-O, and 2 h-mPVDF membranes were 11.16 kg m^{-2} h^{-1}, 11.76 kg m^{-2} h^{-1}, 16.77 kg m^{-2} h^{-1}, and 18.96 kg m^{-2} h^{-1}, respectively. Similarly, the 6 h-mPVDF membrane demonstrated stable flux and permeate conductivity during the test.

It was hypothesized that the membrane's improved flux could be ascribed to the deposition of carboxyl groups on its outer surface, which

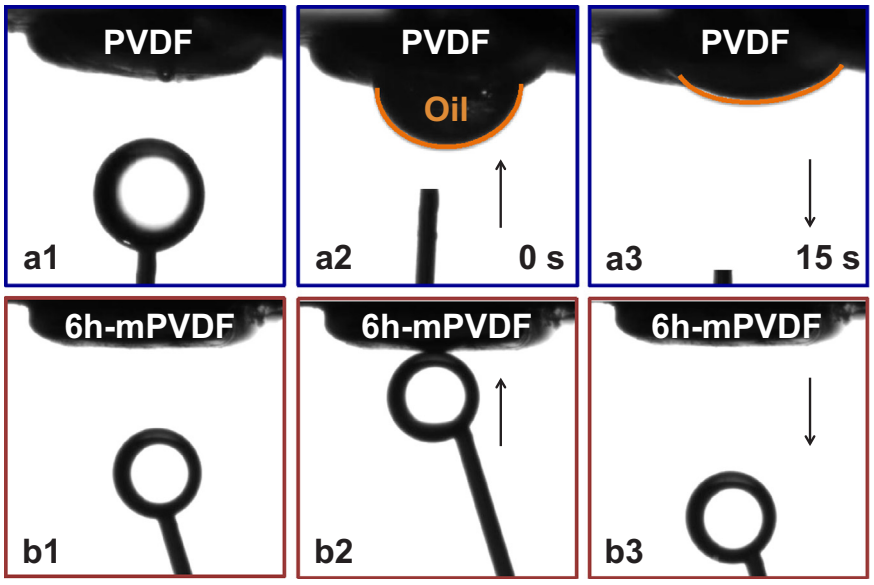

Fig. 6. Captured images of the underwater interactions between petroleum droplets tethered via a needle and the pristine PVDF (a1-a3) and 6 h-mPVDF (b1-b3) membrane surfaces.

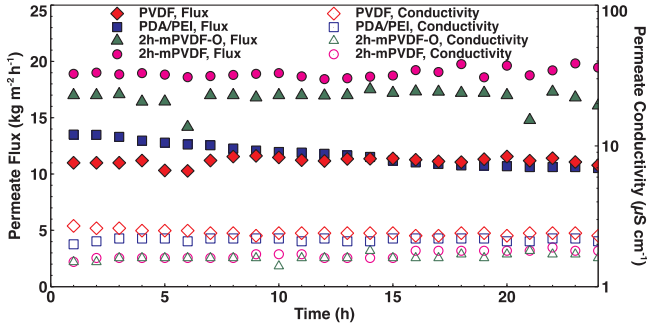

Fig. 7. DCMD performances of the pristine PVDF, PDA/PEI, 2 h-mPVDF-O, and 2 h-mPVDF membranes by feeding 3.5 wt% NaCl. Feed volumetric flow rate (Q_f) = 0.7 L min^{-1}; Permeate volumetric flow rate (Q_p) = 0.25 L min^{-1}; Feed temperature (T_f) = 333 K; Permeate temperature (T_p) = 293 K. Data for the pristine PVDF and PDA/PEI membranes are reproduced with permission from the authors [7,11].

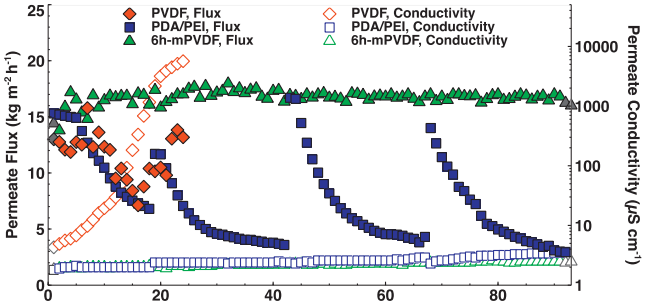

Fig. 9. DCMD performances of the pristine PVDF, PDA/PEI, and 6 h-mPVDF membranes by feeding 50 mg L^{-1} of SDS in 3.5 wt% NaCl. For each experiment, the feed tank was periodically refilled with overflow from the permeate reservoir to maintain the feed concentration. Q_f = 0.7 L min^{-1}; Q_p = 0.25 L min^{-1}; T_f = 333 K; T_p = 293 K. Data for the pristine PVDF and PDA/PEI membranes are reproduced with permission from the authors [7,11].

led to favorable polar-polar interactions with the vapor molecules as illustrated in Fig. 8. This in turn enhanced their adsorption. Subsequently, the hydrophobic PVDF substrate was able to repel both water and non-volatile NaCl solute while insuring that distillate of excellent quality was collected. Finally, the carboxyl groups present on the inner surface of the 2 h-mPVDF membrane served as sites for vapor-liquid interactions, thus leading to faster vapor removal from the substrate pores into the distillate stream [39].

Following the baseline experiments, the fouling and wetting behaviors of the modified PVDF membrane in the presence of 50 mg L^{-1} of anionic (SDS), cationic (DTAB), and non-ionic (Tween® 20) surfactant solutions were analyzed and compared with those of the pristine PVDF and previously reported PDA/PEI coated membranes. As depicted in Fig. 9, these three types of membrane exhibited significantly different fouling and wetting behaviors in the presence of 50 mg L^{-1} of SDS solution. The pristine PVDF membrane experienced severe wetting, as demonstrated by the rapid increase in the permeate conductivity. The PDA/PEI membrane presented reversible fouling but no wetting during the operation. On the other hand, the 6 h-mPVDF membrane demonstrated excellent anti-fouling and anti-wetting properties, maintaining a stable flux and excellent distillate quality throughout the experiment.

The stark difference in the performances of these membranes was believed to be ascribed to their different surface chemistries and wetting properties as well as hierarchical structures, which will be further discussed below. The pristine PVDF membrane is inherently hydrophobic with a smoother surface. The hydrophobic interaction between the hydrophobic tails of SDS unimers and the PVDF membrane surface brought about the adsorption of SDS unimers on the membrane surface, which resulted in pore blockage and severe pore wetting [7]. On the other hand, the PDA/PEI coated membrane had an underwater superoleophobic surface with hierarchical structure. It showed excellent anti-wetting property but poor anti-fouling property in the SDS solution. This could be explained by its surface charge property. The PDA/PEI membrane was tailored in such a way that protonated amine-functional groups were deposited on its surface. The negatively charged SDS unimers would have a natural tendency to adhere on certain regions of the PDA/PEI membrane with the positively charged amine-functional groups, resulting in blockage of the micro-channels within the hierarchical structure. This fouling was reversible and the permeate flux could be recovered by simply washing with Milli-Q® water. Besides that, the deposited PDA/PEI layer offered additional protection to the membrane pores and maintained the liquid entry pressure, rendering them less vulnerable to wetting [11]. Last but not least, the excellent

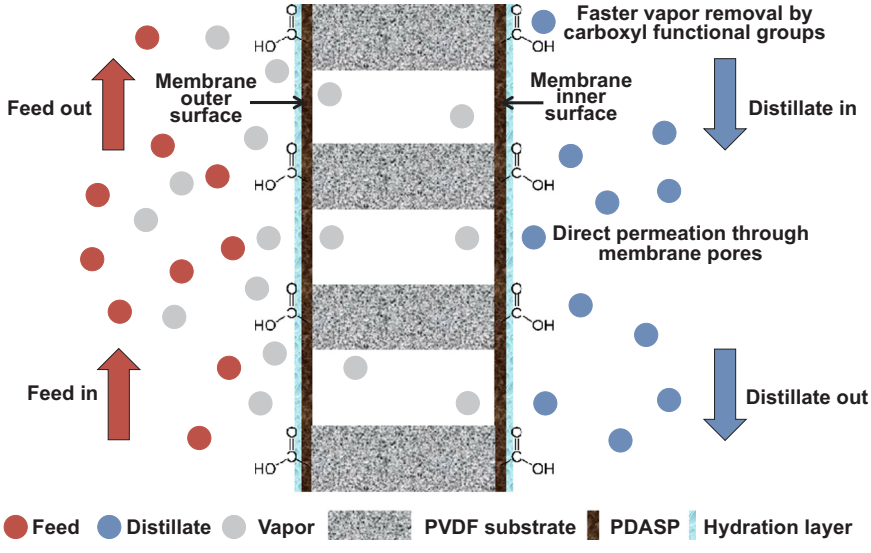

Fig. 8. Schematic diagram of proposed mechanisms for flux enhancement through oxidant-induced surface modification.

fouling- and wetting-resistant properties of the 6 h-mPVDF membrane were ascribed to its underwater superoleophobic surface with hierarchical structures and negative charges, which was able to eliminate both the hydrophobic and electrostatic interactions. Even though protonated amine-functional groups were also detected on the 6 h-mPVDF membrane surface, there were fewer of these groups as compared with the PDA/PEI membrane surface. This was corroborated with the chemical structures of the respective deposited layers [11,27,32]. As such, the electrostatic repulsion between the negatively charged SDS unimers and the negatively charged 6 h-mPVDF membrane surface was more dominant than the electrostatic attraction between these unimers and the protonated amine-functional groups. With fewer SDS unimers adsorbed on its surface, the 6 h-mPVDF membrane remained robust throughout the operation.

In the case of cationic surfactant DTAB, both of the composite membranes (PDA/PEI and 6 h-mPVDF membranes) experience neither fouling nor wetting throughout the entire test duration, which was attested by their respective stable fluxes and high salt rejection rates (> 99.99%). The 6 h-mPVDF membrane presented a relatively higher flux and better distillate quality (final permeate conductivity of 2.2 μS cm^{-1}) as compared to the PDA/PEI membrane (4.3 μS cm^{-1}). Both of these membranes were intrinsically negatively charged but the presence of protonated amine-functional groups could prevent the adsorption of positively charged DTAB unimers. This, coupled with the interfacial hydration layer, could circumvent the issues of fouling and wetting. When the deposited layer comes into contact with the bulk water, water molecules penetrate into its hydrophilic structure to form a hydrogen-bonded network within the deposited layer [40]. Surface hydration leads to an increased resistance against surfactant adsorption, leading to fouling-resistant property. This in turn ensured that the composite membranes remained anti-wetting throughout the test duration. In contrast, the lack of protonated amine-functional groups on the negatively charged and hydrophobic pristine PVDF membrane surface could promote electrostatic attraction as well as hydrophobic interaction between the membrane surface and the DTAB unimers. This in turn led to pore wetting as substantiated by the increase in permeate conductivity. (Fig. 10).

Tween® 20 is one of the most challenging surfactants, with reference to the onset and severity of wetting, as attested by our previous studies [7,11]. In the case of 50 mg L^{-1} Tween® 20, the pristine PVDF membrane was severely wetted, as indicated by the rapid increase in

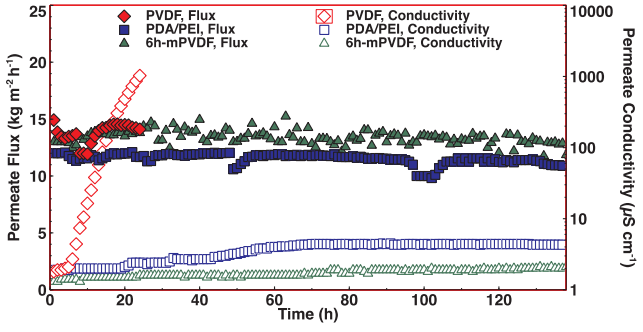

Fig. 10. DCMD performances of the pristine PVDF, PDA/PEI, and 6 h-mPVDF membranes by feeding 50 mg L^{-1} of DTAB in 3.5 wt% NaCl. For each experiment, the feed tank was periodically refilled with overflow from the permeate reservoir to maintain the feed concentration. Q_f = 0.7 L min^{-1}; Q_p = 0.25 L min^{-1}; T_f = 333 K; T_p = 293 K. Data for the pristine PVDF and PDA/PEI membranes are reproduced with permission from the authors [11].

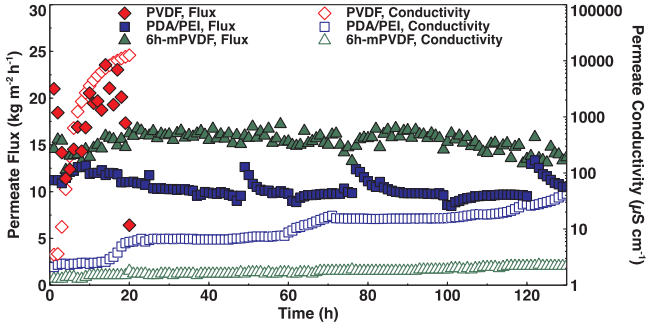

Fig. 11. DCMD performances of the pristine PVDF, PDA/PEI, and 6 h-mPVDF membranes by feeding 50 mg L^{-1} of Tween® 20 in 3.5 wt% NaCl. For each experiment, the feed tank was periodically refilled with overflow from the permeate reservoir to maintain the feed concentration. Q_f = 0.7 L min^{-1}; Q_p = 0.25 L min^{-1}; T_f = 333 K; T_p = 293 K. Data for the pristine PVDF and PDA/PEI membranes are reproduced with permission from the authors [7,11].

permeate flux and conductivity during 20 h of operation as shown in Fig. 11. By contrast, both of the composite membranes (PDA/PEI and 6 h-mPVDF membranes) showed robust stable performances. Moreover, the 6 h-mPVDF membrane outperformed the PDA/PEI membrane, presenting higher permeate flux and better distillate quality. A monolayer of Tween® 20 unimers formed on the hydrophobic PVDF membrane surface via hydrophobic interaction. However, the negative charge on the pristine PVDF membrane would not have contributed to the attachment of this non-ionic surfactant. The adsorbed Tween® 20 unimers on the membrane surface would draw more water molecules towards the membrane pores via their hydrophilic heads, resulting in severe wetting. On the other hand, the formation of hydration layer on the composite membrane surfaces significantly prevented the adhesion of surfactant unimers, maintaining the stable performances of these membranes. The 6 h-mPVDF membrane, with a lower water contact angle of 13.2 ± 2.4°, is more hydrophilic than the PDA/PEI membrane (water contact angle of 25.7 ± 4.0°). The more hydrophilic polar functional groups on the 6 h-mPVDF membrane surface endowed it with a more robust performance as compared to the PDA/PEI membrane.

These three cases involving different types of surfactant solution have demonstrated that composite membranes, such as the 6 h-mPVDF membrane, when endowed with superoleophobic property could effectively overcome fouling and wetting issues in DCMD applications for low surface tension feeds.

3.4.2. *Surfactant-stabilized petroleum-in-water emulsion*

After investigating the challenges of different types of surfactant on the MD performance of the modified PVDF membrane, its feasibility for water recovery from O/W emulsions was studied and the results are shown in Fig. 12. The 500 mg L^{-1} of petroleum-in-water emulsion was prepared by adding Tween® 20 to form a kinetically stable emulsion with mean oil droplet size of less than 10 μm. This serves as an indicator of the applicability of the modified membranes for produced water treatment since removal of fine oil droplets (< 10 μm) is often challenging. As shown in Fig. 12, severe pore wetting was observed for the pristine PVDF membrane, as revealed by the substantial increase in both the permeate flux and conductivity. In contrast, the 6 h-mPVDF showed robust performance throughout the entire operation, presenting a stable flux and excellent distillate quality. The Tween® 20-stabilized petroleum-in-water emulsion had a mean droplet size of 2.16 μm and a near neutral zeta potential of − 3.11 ± 0.32 mV. Thus, the

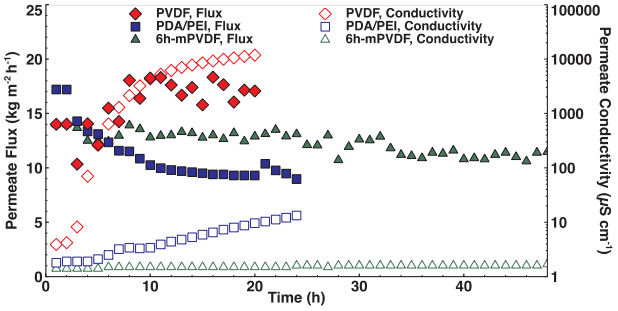

Fig. 12. DCMD performances of the pristine PVDF, PDA/PEI, and 6 h-mPVDF membranes by feeding 500 mg L^{-1} of Tween® 20-stabilized petroleum-in-water emulsion. Fresh emulsions were prepared daily for the respective experiments. Q_f = 0.7 L min^{-1}; Q_p = 0.25 L min^{-1}; T_f = 333 K; T_p = 293 K. Data for the pristine PVDF membrane is reproduced with permission from the authors [7].

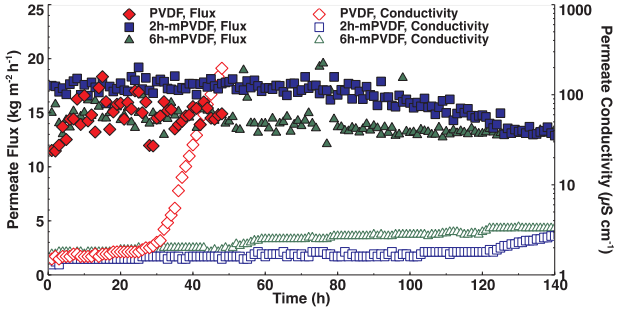

Fig. 13. DCMD performances of the pristine PVDF and mPVDF membranes by feeding seawater. For each experiment, the feed tank was periodically refilled with overflow from the permeate reservoir to maintain the feed concentration. Q_f = 0.7 L min^{-1}; Q_p = 0.25 L min^{-1}; T_f = 333 K; T_p = 293 K.

electrostatic interaction between the petroleum droplets and membrane surface would only have a minor effect on the membrane performance, while the surface wetting property and hierarchical structures play a critical role in governing the fouling and wetting behaviors. The severe wetting behavior of the pristine PVDF membrane was ascribed to its hydrophobic nature, which led to the adsorption of Tween® 20 unimers and petroleum droplets on its surface and/or pores via hydrophobic interaction [7]. The anti-fouling and anti-wetting properties of composite membranes, such as the 6 h-mPVDF membrane, are attributed to the combined effects of the surface superhydrophilicity and hierarchical structures. The hydrophilic moieties (amine-, hydroxyl-, and carboxyl-functional groups) on the deposited PDA layer had the tendency to interact strongly with surrounding water molecules through polar interaction. This strong affinity to water in turn kept the outer surface of the 6 h-mPVDF membrane hydrated and a hydrogen bonded network was formed within the hierarchical structure. Subsequently, the hydration layer provided a significant energetic barrier for the petroleum droplets and Tween® 20 unimers to overcome to be attached onto the surface [11]. This was evidenced by the captive bubble experiments as shown in Fig. 6 and Video S2 in the supplementary material. Water molecules within the interfacial hydration layer possessed low rotational and translational dynamics [41], which could only be displaced from the membrane interface during an unfavorable enthalpy gain episode. Therefore, Tiraferri et al. suggested that maximizing the interfacial energy between the membrane surface and its surrounding water molecules could be an effective anti-fouling strategy [40]. By improving surface hydrophilicity, foulant adhesion tendency is likely to be reduced. As proven in Fig. 12, the more hydrophilic 6 h-mPVDF membrane showed better fouling- and wetting-resistant properties than the PDA/PEI membrane.

3.4.3. Raw seawater

To ascertain that the newly engineered membranes (2 h-mPVDF and 6 h-mPVDF) could be used for real applications, their performances in seawater desalination were analyzed and compared with that of the pristine PVDF membrane as shown in Fig. 13. In the case of the pristine PVDF membrane, no significant fouling was observed and the permeate flux remained fairly constant throughout the test duration. However, pore wetting was first observed after 30 h of operation. The permeate conductivity rose from 1.5 μS cm^{-1} to 196.4 μS cm^{-1} after 48 h of operation, which translated to a salt rejection rate of 99.6%. In contrast, both the 2 h-mPVDF and 6 h-mPVDF membranes produced high quality distillates with final permeate conductivity values at 2.7 and 3.3 μS cm^{-1} after 140 h of operation, respectively (the salt rejection rates were higher than 99.99%). The 2 h-mPVDF membrane presented a higher initial flux than the 6 h-mPVDF membrane. The difference in initial flux could be attributed to the thickness of the deposited layer as observed in Fig. 2(b3) and (c3). The 2 h-mPVDF membrane had a more 'open' structure across its thinner deposited layer. On the other hand, the 6 h-mPVDF membrane had a denser structure across the whole thickness that inevitably provided some mass transfer resistance to vapor flow, albeit small. However, when the deposited layer was thinner and less dense, the membrane became more susceptible to fouling in the long run as exhibited by the 2 h-mPVDF membrane's gradual decline in flux towards the end of the experiment. Hence, there exists a tradeoff between a membrane's robustness and the water recovery rate. A thinner deposited layer may lead to higher initial flux but may not be as robust as a thicker layer in terms of anti-fouling and anti-wetting properties.

4. Conclusions

In this work, we fabricated a composite PVDF hollow fiber membrane with sandwich structure via single-step oxidant-induced dopamine polymerization. In comparison with conventional PDA deposition techniques using dissolved oxygen, this facile and expeditious approach achieved a deposited layer with improved hydrophilicity. The fouling and wetting behaviors of this newly developed membrane in low surface tension saline feeds via bench-scale DCMD experiments were investigated thoroughly. Its performances were compared to those of commercial hydrophobic PVDF and previously reported composite membranes. The novel membrane presented excellent fouling- and wetting-resistant properties against different types of surfactant solution. It also remained robust in O/W emulsion and seawater, during which a stable flux and highly purified distillate were achieved. This could be ascribed to the sustenance of the metastable Cassie-Baxter state within the hierarchical structures formed on the superhydrophilic membrane surface. The deposited layer did not provide additional resistance to vapor transport and instead brought about a flux increment of up to 70% at a feed temperature of 333 K. These results suggest that the newly engineered membrane endowed with underwater superoleophobicity could be used for extended applications of DCMD.

Acknowledgements

This work was funded by the Johnson Matthey Public Limited Company. The authors would also like to acknowledge funding support from the Singapore Economic Development Board to the Singapore Membrane Technology Centre.

Appendix A. Pore size distributions of the pristine PVDF and 6 h-mPVDF membranes

See Fig. A1.

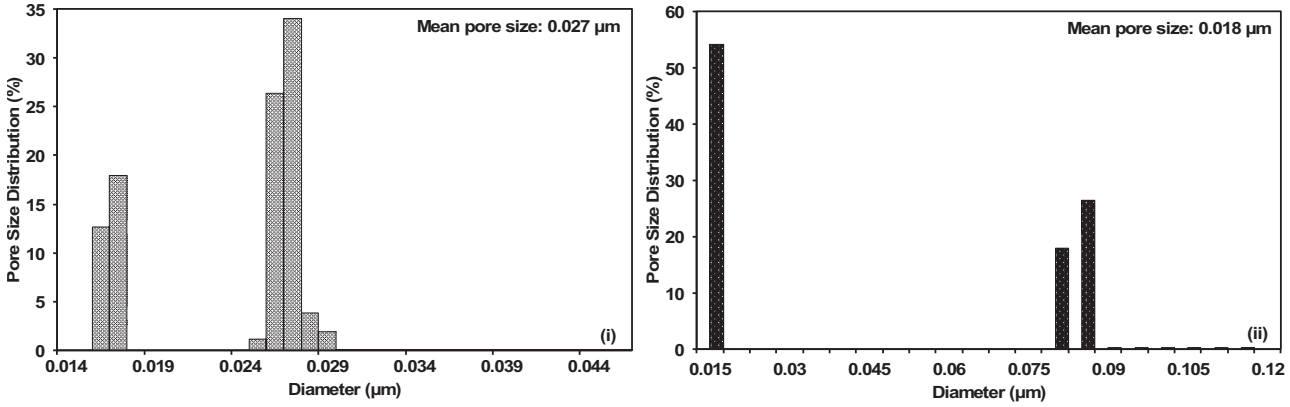

Fig. A1. Pore size distributions of the (i) pristine PVDF and (ii) 6 h-mPVDF membranes.

References

[1] X. Yang, R. Wang, A.G. Fane, Novel designs for improving the performance of hollow fiber membrane distillation modules, J. Membr. Sci. 384 (1–2) (2011) 52–62.

[2] G. Chen, X. Yang, R. Wang, A.G. Fane, Performance enhancement and scaling control with gas bubbling in direct contact membrane distillation, Desalination 308 (2013) 47–55.

[3] Y. Liao, R. Wang, M. Tian, C. Qiu, A.G. Fane, Fabrication of polyvinylidene fluoride (PVDF) nanofiber membranes by electro-spinning for direct contact membrane distillation, J. Membr. Sci. 425–426 (2013) 30–39.

[4] D. Singh, P. Prakash, K.K. Sirkar, Deoiled produced water treatment using direct-contact membrane distillation, Ind. Eng. Chem. Res. 52 (37) (2013) 13439–13448.

[5] F. Macedonio, A. Ali, T. Poerio, E. El-Sayed, E. Drioli, M. Abdel-Jawad, Direct contact membrane distillation for treatment of oilfield produced water, Sep. Purif. Technol. 126 (2014) 69–81.

[6] C. Boo, J. Lee, M. Elimelech, Omniphobic polyvinylidene fluoride (PVDF) membrane for desalination of shale gas produced water by membrane distillation, Environ. Sci. Technol. 50 (22) (2016) 12275–12282.

[7] N.G.P. Chew, S. Zhao, C.H. Loh, N. Permogorov, R. Wang, Surfactant effects on water recovery from oil-in-water emulsions via direct-contact membrane distillation, J. Membr. Sci. 528 (2017) 126–134.

[8] L. Han, Y.Z. Tan, T. Netke, A.G. Fane, J.W. Chew, Understanding oily wastewater treatment via membrane distillation, J. Membr. Sci. 539 (2017) 284–294.

[9] X. Yang, R. Wang, L. Shi, A.G. Fane, M. Debowski, Performance improvement of PVDF hollow fiber-based membrane distillation process, J. Membr. Sci. 369 (1–2) (2011) 437–447.

[10] Y. Liao, R. Wang, A.G. Fane, Engineering superhydrophobic surface on poly(vinylidene fluoride) nanofiber membranes for direct contact membrane distillation, J. Membr. Sci. 440 (2013) 77–87.

[11] N.G.P. Chew, S. Zhao, C. Malde, R. Wang, Superoleophobic surface modification for robust membrane distillation performance, J. Membr. Sci. 541 (2017) 162–173.

[12] A. Tuteja, C. Wonjae, J.M. Mabry, G.H. McKinley, R.E. Cohen, Robust omniphobic surfaces, Proc. Natl. Acad. Sci. USA 105 (47) (2008) 18200–18205.

[13] J. Lee, C. Boo, W.-H. Ryu, A.D. Taylor, M. Elimelech, Development of omniphobic desalination membranes using a charged electrospun nanofiber scaffold, ACS Appl. Mater. Interfaces 8 (17) (2016) 11154–11161.

[14] C. Boo, J. Lee, M. Elimelech, Engineering surface energy and nanostructure of microporous films for expanded membrane distillation applications, Environ. Sci. Technol. 50 (15) (2016) 8112–8119.

[15] Y.C. Woo, Y. Chen, L.D. Tijing, S. Phuntsho, T. He, J.-S. Choi, S.-H. Kim, H.K. Shon, CF4plasma-modified omniphobic electrospun nanofiber membrane for produced water brine treatment by membrane distillation, J. Membr. Sci. 529 (2017) 234–242.

[16] G. Zuo, R. Wang, Novel membrane surface modification to enhance anti-oil fouling property for membrane distillation application, J. Membr. Sci. 447 (2013) 26–35.

[17] Y.-X. Huang, Z. Wang, J. Jin, S. Lin, Novel Janus membrane for membrane distillation with simultaneous fouling and wetting resistance, Environ. Sci. Technol. 51 (22) (2017) 13304–13310.

[18] Z. Wang, S. Lin, The impact of low-surface-energy functional groups on oil fouling resistance in membrane distillation, J. Membr. Sci. 527 (2017) 68–77.

[19] M. Bhadra, S. Roy, S. Mitra, Flux enhancement in direct contact membrane distillation by implementing carbon nanotube immobilized PTFE membrane, Sep. Purif. Technol. 161 (2016) 136–143.

[20] G.A. Polotskaya, A.V. Penkova, A.M. Toikka, Fullerene-containing polyphenylene oxide membranes for pervaporation, Desalination 200 (1–3) (2006) 400–402.

[21] H.-C. Yang, W. Zhong, J. Hou, V. Chen, Z.-K. Xu, Janus hollow fiber membrane with a mussel-inspired coating on the lumen surface for direct contact membrane distillation, J. Membr. Sci. 523 (2017) 1–7.

[22] M. Bhadra, S. Roy, S. Mitra, Nanodiamond immobilized membranes for enhanced desalination via membrane distillation, Desalination 341 (1) (2014) 115–119.

[23] M. Bhadra, S. Roy, S. Mitra, Desalination across a graphene oxide membrane via direct contact membrane distillation, Desalination 378 (2016) 37–43.

[24] C. Zhang, Y. Ou, W.-X. Lei, L.-S. Wan, J. Ji, Z.-K. Xu, CuSO4/H2O2-induced rapid deposition of polydopamine coatings with high uniformity and enhanced stability, Angew. Chem. - Int. Ed. 55 (9) (2016) 3054–3057.

[25] H. Shi, L. Xue, A. Gao, Y. Fu, Q. Zhou, L. Zhu, Fouling-resistant and adhesion-resistant surface modification of dual layer PVDF hollow fiber membrane by dopamine and quaternary polyethyleneimine, J. Membr. Sci. 498 (2016) 39–47.

[26] W. Qiang, Z. Fulong, L. Jie, L. Beijia, Z. Changsheng, Oxidant-induced dopamine polymerization for multifunctional coatings, Polym. Chem. 1 (9) (2010) 1430–1433.

[27] F. Ponzio, J. Barthes, J. Bour, M. Michel, P. Bertani, J. Hemmerle, M. D'Ischia, V. Ball, Oxidant control of polydopamine surface chemistry in acids: a mechanism-based entry to superhydrophilic-superoleophobic coatings, Chem. Mater. 28 (13) (2016) 4697–4705.

[28] B. Wu, F. Hochstrasser, E. Akhondi, N. Ambauen, L. Tschirren, M. Burkhardt, A.G. Fane, W. Pronk, Optimization of gravity-driven membrane (GDM) filtration process for seawater pretreatment, Water Res. 93 (2016) 133–140.

[29] J. Drelich, E. Chibowski, Superhydrophilic and superwetting surfaces: definition and mechanisms of control, Langmuir 26 (24) (2010) 18621–18623.

[30] N.J. Shirtcliffe, G. McHale, S. Atherton, M.I. Newton, An introduction to superhydrophobicity, Adv. Colloid Interface Sci. 161 (1–2) (2010) 124–138.

[31] M. Jin, J. Wang, X. Yao, M. Liao, Y. Zhao, L. Jiang, Underwater oil capture by a three-dimensional network architectured organosilane surface, Adv. Mater. 23 (25) (2011) 2861–2864.

[32] C. Luo, Q. Liu, Oxidant-induced high-efficient mussel-inspired modification on PVDF membrane with superhydrophilicity and underwater superoleophobicity characteristics for oil/water separation, ACS Appl. Mater. Interfaces 9 (9) (2017) 8297–8307.

[33] S.W. Weidman, E.T. Kaiser, The mechanism of the periodate oxidation of aromatic systems. III: a kinetic study of the periodate oxidation of catechol, J. Am. Chem. Soc. 88 (1966) 5820–5827.

[34] H. Lee, S.M. Dellatore, W.M. Miller, P.B. Messersmith, Mussel-inspired surface chemistry for multifunctional coatings, Science 318 (2007) 426–430.

[35] Z. Wang, J. Jin, D. Hou, S. Lin, Tailoring surface charge and wetting property for robust oil-fouling mitigation in membrane distillation, J. Membr. Sci. 516 (2016) 113–122.

[36] D. Breite, M. Went, A. Prager, A. Schulze, Tailoring membrane surface charges: a novel study on electrostatic interactions during membrane fouling, Polymers 7 (10) (2015) 1497.

[37] M. Vaselbehagh, H. Karkhanechi, S. Mulyati, R. Takagi, H. Matsuyama, Improved antifouling of anion-exchange membrane by polydopamine coating in

electrodialysis process, Desalination 332 (2014) 126–133.
[38] S. Kasemset, Z. He, D.J. Miller, B.D. Freeman, M.M. Sharma, Effect of polydopamine deposition conditions on polysulfone ultrafiltration membrane properties and threshold flux during oil/water emulsion filtration, Polymer (U.K.) 97 (2016) 247–257.
[39] M. Bhadra, S. Roy, S. Mitra, A bilayered structure comprised of functionalized carbon nanotubes for desalination by membrane distillation, ACS Appl. Mater. Interfaces 8 (30) (2016) 19507–19513.
[40] A. Tiraferri, Y. Kang, E.P. Giannelis, M. Elimelech, Superhydrophilic thin-film composite forward osmosis membranes for organic fouling control: fouling behavior and antifouling mechanisms, Environ. Sci. Technol. 46 (20) (2012) 11135–11144.
[41] A.M. Dokter, S. Woutersen, H.J. Bakker, Anomalous slowing down of the vibrational relaxation of liquid water upon nanoscale confinement, Phys. Rev. Lett. 94 (17) (2005) (178301-178301).